

# 1 Hybridization load introduced by Alpine ibex hybrid swarms

2

3 F. Gözde Çilingir<sup>1,2+</sup>, Fabio Landuzzi<sup>3+</sup>, Alice Brambilla<sup>2,4</sup>, Debora Charrance<sup>3</sup>, Federica Furia<sup>3</sup>,  
4 Sara Trova<sup>5</sup>, Alberto Peracino<sup>4</sup>, Glauco Camenisch<sup>2</sup>, Dominique Waldvogel<sup>2</sup>, Jo Howard-  
5 McCombe<sup>6</sup>, Yeraldin Chiquinquirá Castillo De Spelozzi<sup>7</sup>, Edoardo Henzen<sup>7</sup>, Andrea Bernagozzi<sup>8</sup>,  
6 Alessandro Coppe<sup>3</sup>, Jean Marc Christille<sup>8</sup>, Manuela Vecchi<sup>5</sup>, Diego Vozzi<sup>7</sup>, Andrea Cavalli<sup>3,9</sup>,  
7 Bruno Bassano<sup>4</sup>, Stefano Gustincich<sup>5,10</sup>, Daniel Croll<sup>11,\*</sup>, Luca Pandolfini<sup>5,10\*\*</sup> and Christine  
8 Grossen<sup>1\*\*\*</sup>

9

10 <sup>1</sup> Swiss Federal Research Institute WSL, Biodiversity and Conservation Biology Research Unit,  
11 Birmensdorf, Switzerland

12 <sup>2</sup> University of Zurich, Department of Evolutionary Biology and Environmental Studies, Zurich,  
13 Switzerland

14 <sup>3</sup> Computational and Chemical Biology, Italian Institute of Technology (IIT), CMP<sup>3</sup>VdA, Aosta, Italy

15 <sup>4</sup> Alpine Wildlife Research Center, Gran Paradiso National Park, Turin, Italy

16 <sup>5</sup> Non-coding RNA and RNA-based therapeutics, Italian Institute of Technology (IIT), CMP<sup>3</sup>VdA,  
17 Aosta, Italy

18 <sup>6</sup> WildGenes Laboratory, Royal Zoological Society of Scotland, Edinburgh, United Kingdom

19 <sup>7</sup> Genomics Facility, Istituto Italiano di Tecnologia (IIT), Genoa, Italy

20 <sup>8</sup> Fondazione Clément Fillietroz ONLUS, Astronomical Observatory of Autonomous Region of  
21 Aosta Valley, Aosta, Italy

22 <sup>9</sup> CECAM-EPFL, Lausanne, Switzerland

23 <sup>10</sup> Non-coding RNA and RNA-based therapeutics, Center for Human Technology, Italian Institute  
24 of Technology (IIT), Genoa, Italy

25 <sup>11</sup> Institute of Biology, University of Neuchâtel, Neuchâtel, Switzerland

26 <sup>+</sup> These authors equally contributed to the work

27 <sup>\*</sup>co-corresponding authors (daniel.croll@unine.ch, luca.pandolfini@iit.it,  
28 christine.grossen@wsl.ch)

29 lead contact (christine.grossen@wsl.ch)

## 30 **Summary**

31 Species restoration efforts can be threatened by the accumulation of deleterious mutations and  
32 inbreeding depression associated with the historic population contraction. However, even  
33 successfully restored species could face deleterious mutation swamping from hybridization with  
34 an abundant and closely related species. Here, we analyze this risk for Alpine ibex (*Capra ibex*),  
35 a flagship species of large mammal restoration in the Alps. The Alpine ibex faced near-extinction  
36 two centuries ago, resulting in exceptionally low genome-wide diversity and increased inbreeding,  
37 which facilitated the purging of severe deleterious mutation load. For this, we produced a highly  
38 contiguous chromosome-level genome assembly of the Alpine ibex capturing structural  
39 divergence from domestic goat (*Capra hircus*) and mapping immune-relevant MHC genes.  
40 Analyses of eight recent ibex-goat hybrids from two swarms in Northern Italy, combined with 29  
41 non-hybrid Alpine ibex and 22 domestic goats, identified 215 masked loss-of-function (LOF)  
42 mutations introduced via hybridization. Yet, we found no evidence for counter-selection in early  
43 backcrosses. This exposes Alpine ibex to further backcrosses compounding the deleterious  
44 mutation load of the species by a factor of up to two. Our work provides one of the first direct  
45 estimates of hybridization load and guides conservation efforts to preserve endangered species  
46 gene pools.

47  
48 **Keywords:** conservation genetics, deleterious mutation load, anthropogenic hybridization, hybrid  
49 swarm, hybridization load, heterosis, Alpine ibex

50

51

## 52 Results and discussion

53 Human activity has profoundly affected species and populations through habitat degradation and  
54 over-exploitation leading to severe population reductions and extinctions <sup>1</sup>. A particular concern  
55 for species conservation is increased levels of inbreeding and the expression of deleterious  
56 mutations in small populations. Recent studies provided compelling evidence for changes in  
57 deleterious mutation load in natural populations (reviewed in Dussex et al. <sup>2</sup>; Robinson et al. <sup>3</sup>).  
58 As predicted by theory, population bottlenecks were repeatedly shown to lead to the selective  
59 removal (purging) of highly deleterious (usually recessive) mutations, while less severely  
60 deleterious mutations can accumulate (e.g., Xue et al.<sup>4</sup>, Grossen et al. <sup>5</sup>, Dussex et al. <sup>6</sup>; reviewed  
61 in Dussex et al. <sup>2</sup>). Mutation load is defined as load resulting from newly introduced deleterious  
62 mutations <sup>7</sup>. Empirical assessments of fitness effects confirmed the detrimental impact of mutation  
63 load and inbreeding on both individual and population fitness <sup>8,9</sup>. However, the origin of deleterious  
64 mutations remains often unresolved. In addition to *de novo* mutations, a potentially significant  
65 source of mutation load could be deleterious variants introduced into a population through  
66 hybridization.

67  
68 Hybridization in nature contributes to genetic variation and fosters adaptation <sup>10,11</sup>. Hybridization  
69 in bottlenecked species may introduce new adaptive genetic variation, compensating previously  
70 lost variation <sup>12</sup>. In addition, high levels of heterozygosity in hybrids can also initially mask  
71 deleterious mutations, thereby causing hybrid vigor (*i.e.*, heterosis) and mitigating inbreeding. Yet,  
72 this initial masking of deleterious mutations prevents their counter-selection in early generations.  
73 Hybridization also poses the risk of disrupting local adaptation through introgression of non-native  
74 alleles, in particular if the new species contact is caused by human activities <sup>13–15</sup>. Such  
75 introduction of deleterious mutations is defined as hybridization load <sup>12</sup>. Overall, deleterious  
76 mutations played a significant role in hybridization events in animals such as fish <sup>16,17</sup>, plants  
77 including crops <sup>18–20</sup>, and trees <sup>21</sup>. These studies indicate that while hybridization can introduce  
78 beneficial alleles, linked deleterious variants can reduce fitness and create partial barriers to  
79 introgression. The interplay of adaptive and maladaptive variation introduced through  
80 hybridization is likely complex and poorly understood.

81  
82 As hybridization can introduce new adaptive genetic variation and alleviate the effects of  
83 inbreeding through hybrid vigour, genetically impoverished species may be particularly  
84 susceptible to the introduction of hybridization load. To quantify load in genomes and to predict  
85 effects of introgression, high-quality genomic resources are essential <sup>22</sup>. The Alpine ibex (*Capra*

86 *ibex*), a mountain ungulate endemic to the European Alps (Figure 1A, B), has experienced severe  
87 bottlenecks since the early 19th century and repeated hybridization events<sup>12,23,24</sup>. However, the  
88 evolution of deleterious mutation load driven by hybridization remains poorly understood.

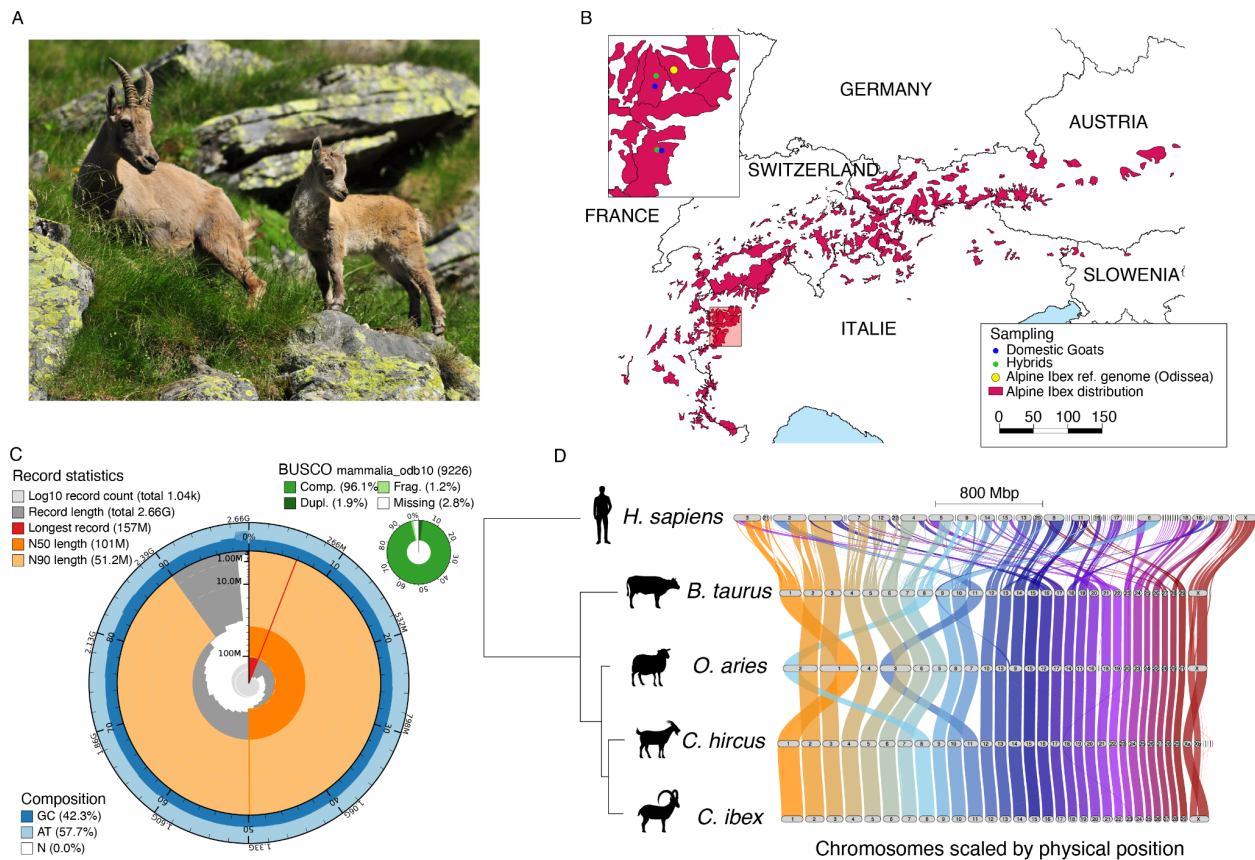
89  
90 Conservation efforts have restored the species to its original distribution area, with a current  
91 population of about 55,000 individuals<sup>25</sup>. However, these bottlenecks have resulted in Alpine ibex  
92 having one of the lowest levels of genetic variation among mammals<sup>5,26</sup>. This reduced genetic  
93 diversity has led to increased inbreeding and inbreeding depression, with negative effects both at  
94 the individual<sup>27</sup> and population level<sup>28</sup>. Severe genetic load was likely reduced through purging  
95 of highly deleterious mutations, while less severe mutations accumulated<sup>5</sup>. Genome-wide  
96 analyses showed that successful hybridizations with domestic goats (*Capra hircus*) likely occurred  
97 during the severe historic bottleneck when ibex numbers were at their lowest<sup>29,30</sup>. Introgression  
98 was particularly evident at immune-relevant genes, where genetic variability in Alpine ibex is very  
99 low. Such introgressed variants may have been under positive selection due to heterozygote  
100 advantage at immune loci<sup>29</sup>. However, hybridization is also expected to have detrimental  
101 consequences for Alpine ibex, with potential loss of adaptations to the alpine environment and  
102 the introduction of deleterious variants. Of particular concern are the recently discovered hybrid  
103 swarms between Alpine ibex and domestic goats in Northern Italy<sup>24,31</sup>. Such populations of  
104 hybrids have survived beyond the initial hybrid (F1) generation, and there is continued  
105 backcrossing between hybrid individuals and parental species<sup>24</sup>. This extensive hybridization  
106 raises concerns of maladaptation and loss of ibex identity. Here, we generated the first reference-  
107 quality genome for Alpine ibex to quantify the hybridization load generated by high rates of  
108 hybridization as observed in hybrid swarms.

109

### 110 **A high-quality chromosome-level assembly**

111 We assembled a chromosome-level genome of a wild female Alpine ibex (Odissea) from the Gran  
112 Paradiso National Park population (Lauson Valley, Cogne, Italy). Using 130 Gb of high-quality  
113 ONT data, we generated a 2.66 Gb draft genome with 1040 contigs (N50 58.7 Mb), polished with  
114 short read sequencing data. The contigs showed high completeness, with BUSCO and k-mer-  
115 based scores of 96.1% and 98.6%, respectively (Figure 1C). We generated Hi-C data to anchor  
116 contigs into 30 pseudo-chromosomes (Figure S1) with a resulting N50 of 101.2 Mb and matching  
117 the chromosome numbers of domestic goats<sup>32</sup> (Table S1, Figure 1D). The Alpine ibex assembly  
118 also includes the full mitochondrial genome (16.7 Kb, Figure S2). The nuclear genome is  
119 constituted of 43.4% repetitive elements (1.15 Gb), dominated by retroelements (38.22%),

120 including Long Interspersed Nuclear Elements (LINEs: 32.56%) and Long Terminal Repeats  
 121 (LTRs: 4.87%) (Table S2). We integrated gene model evidence using transcriptome-assisted  
 122 predictions as well as annotations lifted over from the sheep (*Ovis aries*) genome, yielding a  
 123 BUSCO completeness of 99.7% at the transcript level (Table S3). The annotated gene set  
 124 consisted of 32,783 protein-coding genes and 61,420 transcripts (Table S4).  
 125



126 **Figure 1: Sampling and genome description.** A) Picture of a female Alpine ibex with her  
 127 offspring (photo by Dario de Siena, Archivio PNGP). B) Map of species distribution and zoom in  
 128 on the sampling location of Odissea (shown in yellow), the hybrids (green), and domestic goats  
 129 (blue). C) Snail plot visualizing assembly statistics: scaffold statistics, sequence composition  
 130 proportions, and BUSCO completeness scores. D) Riparian plot showing the results of the gene  
 131 synteny analysis conducted on the cattle, sheep, domestic goat, and Alpine ibex genomes using  
 132 GENESPACE. The human genome was used as an outgroup. See also Figures S1-S4.  
 133

134

135

136 **Recent structural variants arising in Alpine ibex**

137 We used gene order conservation analyses between Alpine ibex and three related domesticated  
138 mammals, including cattle (*Bos taurus*), sheep (*Ovis aries*), and domestic goat, as well as the  
139 human genome as an outgroup to detect chromosomal rearrangements (Figure 1D; Tables S5  
140 and S6). Chromosomal synteny is largely conserved between the domestic goat and the Alpine  
141 ibex. The sheep genome experienced three chromosome fusions, combining in each two distinct  
142 chromosomes found in cattle and goats. The Alpine ibex genome includes a fully assembled X  
143 chromosome compared to the domestic goat (contigs Xa and Xb; Figure 1D). In addition, the  
144 Alpine ibex chromosomes 12 and 17 also include sequences matching to unplaced contigs in  
145 domestic goat. Overall, domestic goat and Alpine ibex genomes share 2.4 Gb of syntenic regions  
146 (~90.2%). Structural variant analyses with SyRI confirmed major rearrangements on  
147 chromosomes 7, 18, and 23 (Figure S3, S4A), mainly involving indels (38 Mb, 1.4% of the  
148 genome) and inversions (49 Mb, 1.8%), with fewer duplications and translocations (Figure S4B,  
149 C). Highly divergent regions (HDR) covered a total of 43 Mb (1.6%; Figure S4B, C). Nearly half  
150 (45%) of all insertions, deletions, and HDRs between domestic goat and Alpine ibex overlapped  
151 with gene bodies, and the proportion was even higher for inversions (52%), duplications (54%),  
152 and translocations (78%).

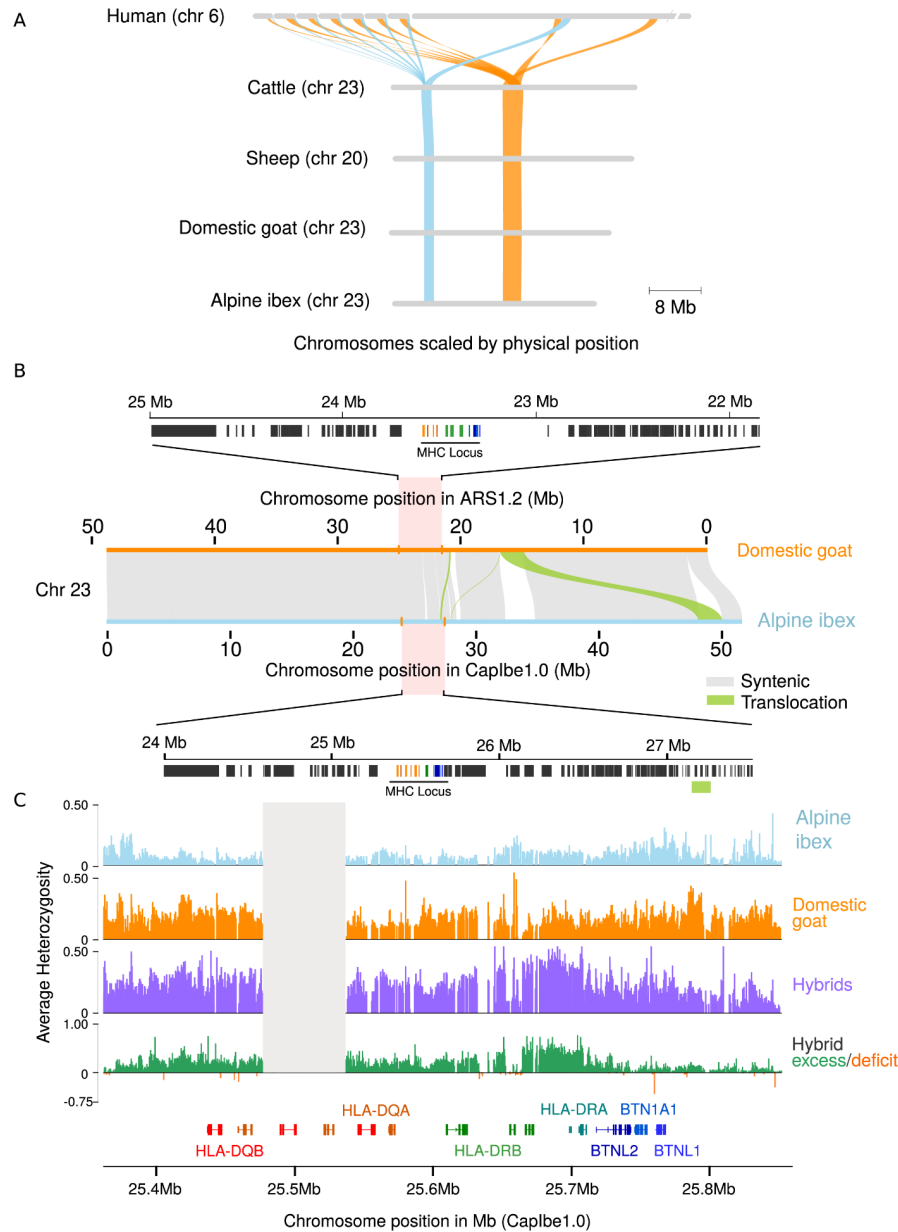
153

#### 154 **MHC conservation and high heterozygosity in recent hybrids**

155 High levels of polymorphisms at the major histocompatibility complex (MHC) are typically favored  
156 within species, and the locus is prone to duplications<sup>33</sup>. Consequently, assembling the MHC  
157 regions can be challenging [see e.g., challenges for human MHC assembly<sup>34–36</sup>]. Here, we report  
158 a contiguous assembly of the Alpine ibex MHC. High-level synteny is well-conserved among  
159 cattle, sheep, domestic goat, and Alpine ibex in both their main MHC regions (class I and II, Figure  
160 2A). We detected a ~110 kb translocation between Alpine ibex and the domestic goat near the  
161 MHC class II cluster that does not affect MHC coding sequences (Figure 2B). An additional  
162 translocation of ~1.92 Mb occurred further away from the MHC class II on chromosome 23 (Figure  
163 2B). In contrast to the human MHC, both the domestic goat and Alpine ibex MHC class II clusters  
164 encode DR- and DQ-genes but no DP-genes<sup>37,38</sup>. The DR- and DQ-genes are generally  
165 exceptionally polymorphic. Over 100 DRB1 alleles for sheep and dozens for goats have been  
166 deposited in GenBank, reflecting their crucial role in immune diversity. Alpine ibex populations  
167 have previously been shown to carry introgressed alleles from the domestic goat at the DRB gene  
168<sup>30</sup> and other immune-related genes<sup>29</sup>.

169

170 To assess whether hybridization load may pose a risk to Alpine ibex, we generated whole-genome  
171 sequencing data of eight recent hybrid individuals sampled from two hybrid swarms in Northern  
172 Italy<sup>24</sup> and four domestic goats representing the local breed, and collected in the same areas as  
173 the hybrids (Table S7). We analysed the new sequencing data together with publicly available  
174 data representing 29 non-hybrid Alpine ibex as well as 18 domestic goats. Average individual  
175 heterozygosity was consistently low in non-hybrid Alpine ibex individuals compared to hybrids  
176 and domestic goats, including particularly striking contrasts in the DR- and DQ-gene regions  
177 (25.40-25.75 Mb; Figure 2C). Diversity at the MHC is associated with disease resistance in a  
178 number of species<sup>39-45</sup>, including Alpine ibex<sup>46</sup>. The high diversity at the MHC in hybrids may  
179 therefore confer a selective advantage under disease pressure. Hence, hybridization and MHC  
180 introgression may be favored in the wild, posing a risk of disrupting local adaptation in wild Alpine  
181 ibex.



182  
183 **Figure 2: Conserved synteny at the MHC and high diversity in hybrids.** A) Close-up of the  
184 synteny analysis, conducted with GENESPACE, highlighting two MHC regions within Alpine ibex  
185 chromosome 23 (light blue and orange, respectively).  
186 B) Structural variation along chromosome 23 based on SyRI, including annotations of domestic  
187 goat (top) and Alpine ibex (bottom) in the range encompassing the major MHC II region.  
188 C) Average individual heterozygosity is shown as observed heterozygosity in Alpine ibex (blue),  
189 domestic goat (orange), and hybrids (purple). Heterozygosity excess and deficit in hybrids are  
190 shown with green (positive values) and orange (negative values), respectively. The grey box  
191 highlights a region corresponding to 25.47-25.55 Mb (encoding *DQA* and *DQB*), which showed a

192 local lack of coverage in domestic goats while being evenly covered in Alpine ibex (except for  
193 Alpine ibex individuals with previously reported historic introgression in the MHC region, see  
194 Figures S5-11 and Grossen et al.<sup>30</sup>).

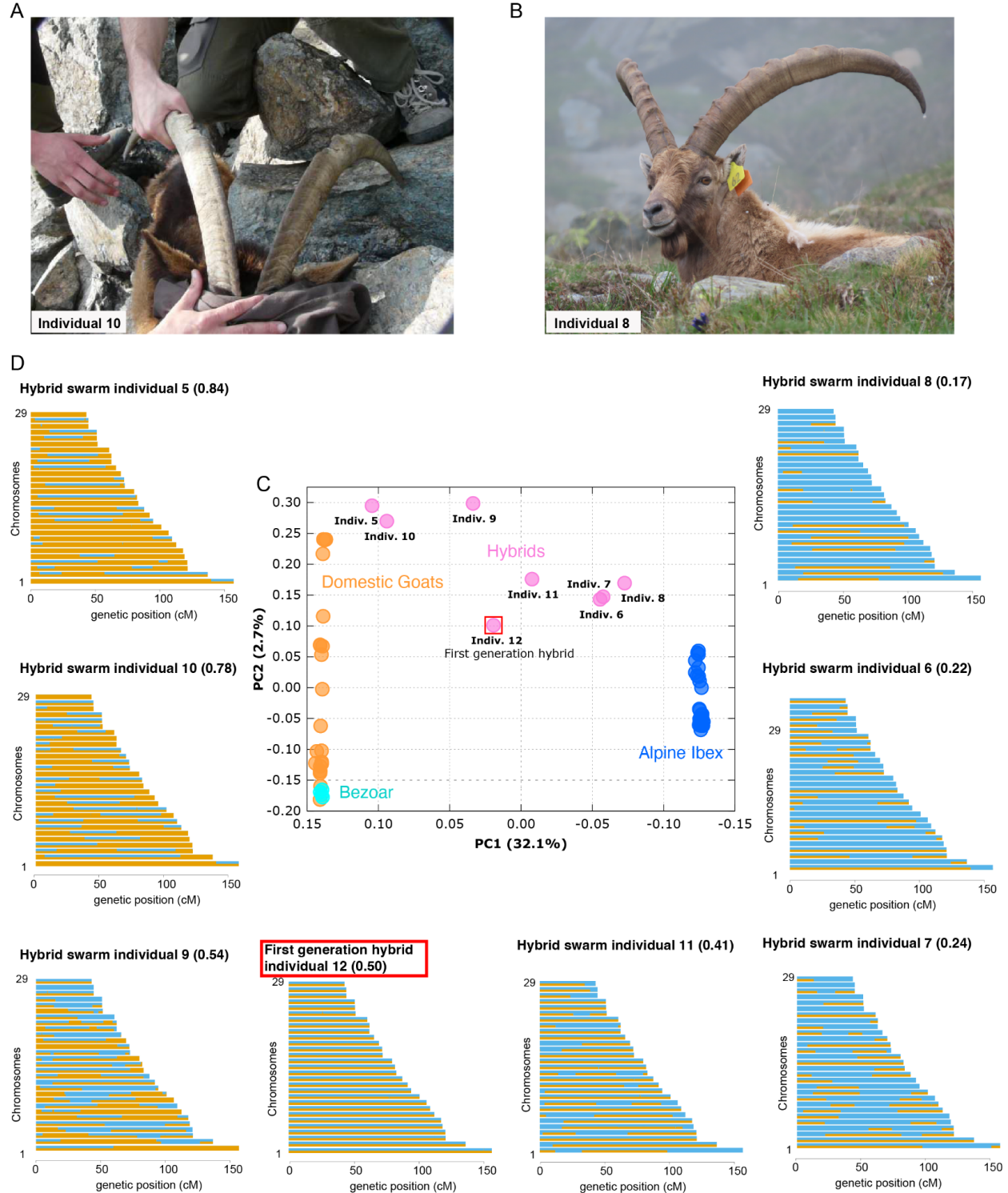
195

### 196 **Emerging recombinant haplotypes in an Alpine ibex hybrid swarm**

197 The recent observation of hybrid swarms in Northern Italy renewed concerns about Alpine ibex  
198 conservation efforts<sup>24</sup>. The high collinearity of Alpine ibex and domestic goat genomes should  
199 facilitate recombination between haplotypes. At the phenotypic level, recent hybrids carry well-  
200 recognizable domestic goat features such as horn shape and fur coloration<sup>24</sup> (Figure 3A, B). We  
201 analyzed the whole-genome sequencing data to recapitulate introgression patterns in two hybrid  
202 swarms. We furthermore sequenced four domestic goat individuals from the same two regions  
203 (Figure 3, Table S7). Non-hybrid individuals of each species showed clear separation based on  
204 a principal component analysis (PCA,  $n = 29$  Alpine ibex,  $n = 22$  domestic goats; Figure 3C)  
205 performed on 86,650 biallelic SNPs. All eight hybrid swarm members showed clear evidence for  
206 recent admixture (Figure 3C). Next, we performed chromosome painting using genome-wide  
207 polymorphism of the hybrids to identify parental contributions. Individual 12 matched expectations  
208 for a F1 hybrid with uninterrupted goat and Alpine ibex haplotypes over all chromosomes (Figure  
209 3D). Hybrids that underwent backcrosses revealed evidence for recombination events as  
210 interrupted haplotypes (Figure 3D). Genome-wide ancestry matched well with recombination  
211 patterns and parental haplotype contributions. Individual 5 showed both the highest degree of  
212 ancestry and the largest haplotypes of domestic goat. In contrast, individual 8 carried the longest  
213 Alpine ibex haplotype blocks consistent with its strong Alpine ibex ancestry (Figure 3D). The  
214 highly diverse set of recombinants in the Alpine ibex swarm raises significant concerns for further  
215 introgression in the two respective regions and other populations with a high incidence of contacts  
216 between domestic goat and Alpine ibex.

217

Figure 3



218

219 **Figure 3: Genome-wide patterns of hybridization**

220 A) Picture of hybrid individual 10. B) Picture of hybrid individual 8. C) Principal Component

221 Analysis of biallelic autosomal SNPs showing the clustering of species and the distribution of

222 hybrids along the conjunction between Alpine ibex and domestic goat/bezoar. D) Chromosome

223 paintings drawn with Mosaic, ordered according to the proportion of domestic goat ancestry  
224 (decreasing proportion of goat genome shown in orange from left to right).

225

### 226 **Hybridization load in two Alpine ibex hybrid swarms**

227 We assessed the extent of hybridization load, which could be introduced into Alpine ibex through  
228 a hybrid swarm. The cross-species polymorphism included 59,544,737 SNPs of which 0.009%,  
229 0.311%, and 0.499% were classified as having putatively high, moderate, and low impacts on  
230 encoded proteins, respectively (see also Tables S8 and S9). High-impact variants, such as those  
231 causing premature stop codons or frameshifts, are predicted to severely disrupt protein function  
232 (e.g., loss-of-function, LOF variants). Moderate and low impact variants cover, respectively,  
233 missense mutations that may alter protein structure without severe impairment and synonymous  
234 changes with minimal expected effects on protein function. To evaluate the robustness of  
235 predicted high-impact mutations, we tested whether these mutations were disproportionately  
236 located in potential pseudogenes. However, we found that the presence of deleterious mutations  
237 cannot be explained by pseudogene-like regions alone (Table S10).

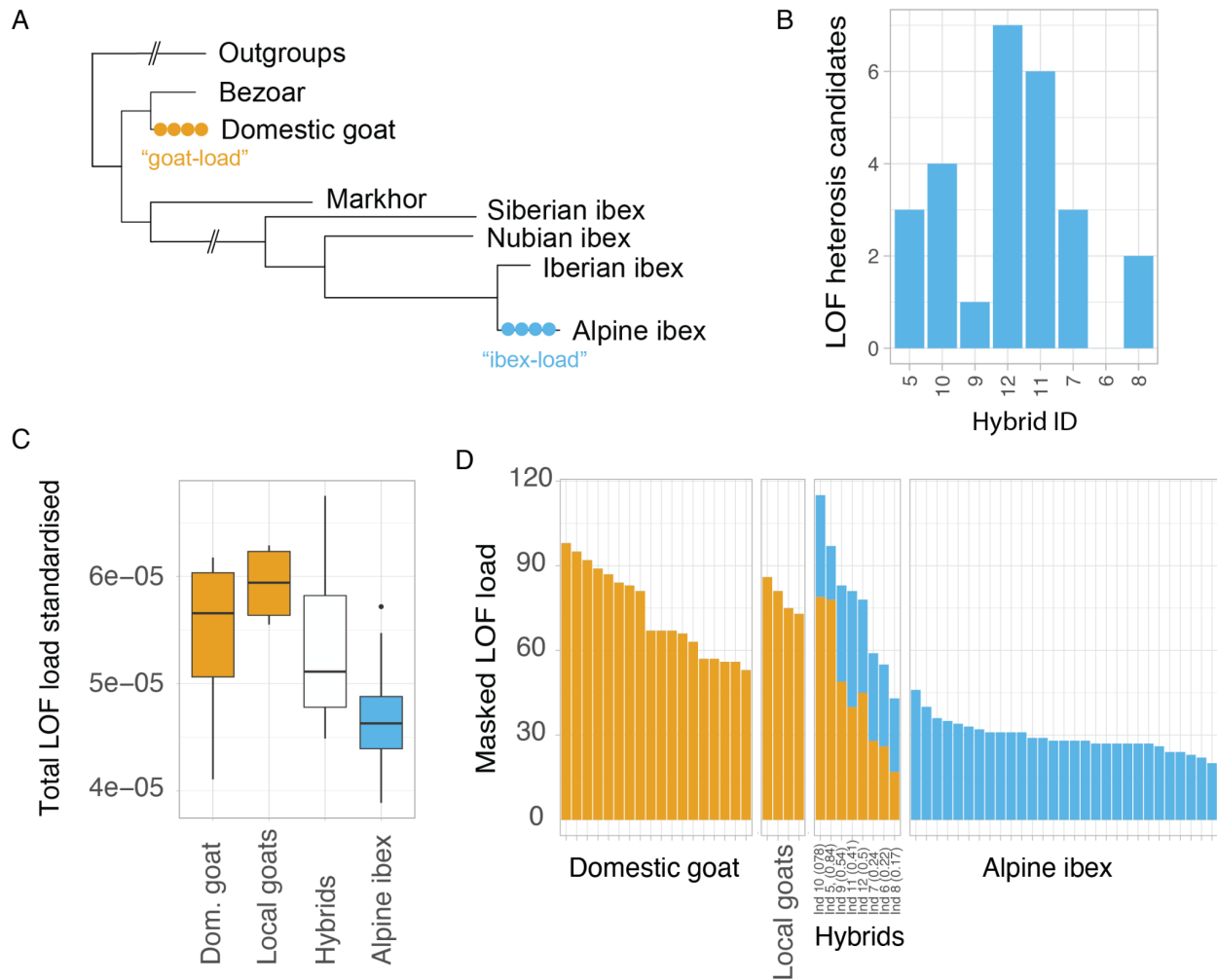
238

239 We investigated deleterious mutations derived from either domestic goat or Alpine ibex as a proxy  
240 for genetic load (Figure 4A). First, we analyzed candidate mutations underpinning heterosis in  
241 hybrids. We defined these mutations as fixed derived LOF variants in Alpine ibex (fixed for the  
242 ancestral allele in all other species). Seven LOF variants were identified as candidates for  
243 heterosis (Table S11). Severely disruptive variants such as LOF are generally recessive; hence,  
244 these should be masked in the heterozygous state, conferring increased fitness (heterosis) in  
245 hybrids compared to non-hybrid Alpine ibex. We found that the analyzed hybrids each carried  
246 between zero and all seven candidates for heterosis in the heterozygous state (in a backcrossed  
247 individual into Alpine ibex and a F1 hybrid, respectively, Figure 4B). This suggests that the positive  
248 effects of masking LOF variants in hybrids may quickly get lost through backcrossing. The  
249 observed signs of hybrid vigour in Alpine ibex-domestic goat hybrids<sup>24</sup> may reflect a combination  
250 of such masking effects alongside other genetic (e.g., overdominance) or epigenetic factors<sup>47</sup>.

251

252

Figure 4



253

254 **Figure 4: Deleterious mutation load in hybrids**

255 A) Phylogenetic tree showing species relationships and the definition of “goat-load” and “ibex-  
 256 load” defined as newly derived mutations private to the respective species. B) Counts of loss-of-  
 257 function alleles found in the heterozygous state for each sequenced hybrid individual (ordered  
 258 according to proportion of goat). C) Total counts of loss-of-function alleles standardized by the  
 259 total counts of modifier alleles. Box plots per species. Local goats refer to domestic goat breeds  
 260 kept in the region where hybrid swarms were detected. See also Figure S12. D) Masked loss-of-  
 261 function load (heterozygote counts) per individual. Local goats, as in C.

262

263 We also investigated the extent to which hybridization load could affect Alpine ibex. We found  
 264 that the mutation load for LOF variants (standardized by neutral variation) was higher in domestic  
 265 goat than in Alpine ibex (Figure 4C,  $p < 10^{-9}$ ). As a consequence, hybrids carried a total of 215  
 266 newly acquired LOF variants (Table S11), more than doubling the total number of LOF variants

267 in Alpine ibex ( $n = 177$  LOF variants detected among 29 non-hybrid Alpine ibex). With an average  
268 of 76 masked LOF variants per hybrid individual compared to 29 in non-hybrid Alpine ibex, hybrids  
269 carried on average a 2.5 times higher severe masked load (Figure 4D). Hybrids backcrossed with  
270 Alpine ibex saw their mutation load decreased with each generation as expected (Figure 4D). Yet  
271 standardized LOF load did not decrease over the first few generations of back-crossing into Alpine  
272 ibex (Figure S12). Hence, there is no indication that selection acted to reduce mutation load. Such  
273 counterselection is expected to face less interference after further back-crossings (and  
274 recombination). Since the hybrid swarm acquired hybridization load (*i.e.*, masked mutation load),  
275 our data highlights that Alpine ibex are at risk of increasing their mutation load through leakage  
276 from the hybrid swarm.

277

## 278 **Concluding remarks**

279 The detrimental effects of deleterious variants are well-recognized as a risk factor in endangered  
280 species <sup>2,3</sup>. While a large number of recent studies investigated the evolution of deleterious  
281 mutation load as a consequence of small population size<sup>4–6,48–52</sup>, much less consideration was  
282 given to the source of deleterious mutation load. Here, we investigated the role of hybridization  
283 with domestic goat as a source of mutation load for Alpine ibex. The high heterozygosity in hybrids  
284 may confer early-generation hybrids an advantage over non-hybrid individuals, compounding the  
285 risk of further introgression and a potential loss of local adaptation. Here, we show that high rates  
286 of hybridization can introduce deleterious mutations from a closely related species without evident  
287 counterselection. Given the increased rate of human-induced hybridization <sup>53</sup>, tracking the  
288 deleterious effects of hybridizations should be a crucial element of species conservation actions.

289

## 290 **Resource availability**

### 291 **Lead contact**

292 Further information and requests for resources and reagents should be directed to, and will be  
293 fulfilled by, the lead contact, Christine Grossen (Christine.Grossen@wsl.ch).

294

### 295 **Materials availability**

296 This study did not generate novel biological materials.

297

### 298 **Data and code availability**

299 Raw sequencing experiment data were submitted to the SRA archive under the project identifier  
300 PRJNA1104824 (reviewer link:

301 <https://dataview.ncbi.nlm.nih.gov/object/PRJNA1104824?reviewer=kij4fipl6g0eheslrgertb0ak9>).

302 The final *C. ibex* genome assembly and high-confidence coding gene annotations will be publicly  
303 available in the NCBI repository XXXXXX (currently undergoing NCBI processing). The

304 *Caplbe1.0* genome fasta file, full transcriptome models, gene functional annotation, and GERP

305 scores relative to the novel genome can be downloaded from Zenodo

306 (<https://doi.org/10.5281/zenodo.15632776>; <https://doi.org/10.5281/zenodo.15632854>;

307 <https://doi.org/10.5281/zenodo.15357984>).

308 This paper does not report original code. The lead contact can provide any additional information  
309 required to reanalyze the data reported in this paper upon request.

310

## 311 **Acknowledgments**

312 For domestic goat sampling, we thank Stefania Zanet, Alice Naudin, and Emilio Gugliermetti. For

313 hybrid sampling, we thank the Surveillance Service of Gran Paradiso National Park, the Forestry

314 Service of Regione Valle d'Aosta, Claudio Scaini, and the personnel of Città Metropolitana di

315 Torino and of CATO4, Noel Zehnder and Luca Rossi. We thank Sara Gottardo, Francesca

316 Groppo, and the sequencing facility of CMP<sup>3</sup>VdA in Aosta for technical assistance with Illumina

317 whole-genome sequencing. We thank Sergio Decherchi, Alessandro Parodi, and Mattia Pini for

318 their support for high-performance computing and data storage, and Dario de Siena and Raffaele

319 Turvani for the beautiful ibex pictures.

320 F. Gözde Çilingir was funded by the Swiss National Science Foundation (IZCOZO\_198147 to A.B.

321 and C.G. and 31003A\_182343 to C.G.).

322 This work was supported by the 5000genomi@VdA Project co-founded by “Fondo Europeo di

323 Sviluppo Regionale (FESR CUPB68H19005520007) to SG and AC; FL, ST, ACa, MV and LP

324 were supported by “Fondo Europeo di Sviluppo Regionale (FESR CUPB68H19005520007); DC

325 and FF were recipient of a fellowship from Programma Investimenti per la crescita e l'occupazione

326 2014/20” (European Social Fund, ESF CUP B65F19001200009) and continued their activity with

327 a fellowship from Programma Regionale Fondo Sociale Europeo Plus 2021/2027 (“European

328 Social Fund”, ESF CUPJ51B24000170002).

329 This work is part of the "Technologies for Sustainability" Flagship program of IIT (L.P.).

330

## 331 **Author contributions**

332 AB conceived the study and managed DNA sample collection. AB, AP, GC, DW, JHM, and BB  
333 performed and coordinated the sampling. FGÇ, FL, DC, LP, and CG designed experiments and  
334 analyses. EH, YCCDS, and DV generated sequencing data under the supervision of FGÇ, LP,  
335 MV, and ST. FGÇ, FL, FF, LP, and CG performed analyses with input from DC. FGÇ, FL, AB,  
336 DC, LP, and CG wrote the manuscript with contributions from all authors. JMC, ACa, SG, AB, and  
337 CG provided funding and resources for the study.

338

### 339 **Declaration of interests**

340 The authors declare no competing interests.

341

### 342 **Supplemental information**

343 **Document S1** contains Figures S1–S12.

344 **Figure S1:** HiC contact map showing the data used for genome scaffolding, related to Figure 1.

345 **Figure S2:** Scheme of the Alpine ibex mitochondrial genome, related to Figure 1.

346 **Figure S3:** Structural variant calling between domestic goat and Alpine ibex (based on SyRI)  
347 across all 29 autosomes, related to Figure 1.

348 **Figure S4:** Major translocations between domestic goat and Alpine ibex observed on  
349 chromosomes 7 and 18 based on SyRI. B) Total counts and cumulative sizes of the structural  
350 variants identified by SyRI between the Alpine ibex and domestic goat genomes. C) Size  
351 distribution of translocations shown as a histogram from the same variants as in A (INDEL:  
352 insertion/deletion, INV: inversion, DUP: duplication, TRANS: translocation, HDR: highly divergent  
353 region), related to Figure 1.

354 **Figure S5:** Read depth profiles of already available whole genome sequencing samples of Alpine  
355 ibex (N=29), domestic goat (N=18), Iberian ibex (N=4), and 12 newly sequenced individual  
356 samples (domestic goat, N=4; hybrids, N=8). The profiles are displayed for the genomic interval  
357 25.47-25.55 Mb on chromosome 23, which includes portions of *DQA* and *DQB* loci, related to  
358 Figure 2.

359 **Figure S6:** Figure S5 continued, related to Figure 2.

360 **Figure S7:** Figure S5 continued, related to Figure 2.

361 **Figure S8:** Figure S5 continued, related to Figure 2.

362 **Figure S9:** Figure S5 continued, related to Figure 2.

363 **Figure S10:** Figure S5 continued, related to Figure 2.

364 **Figure S11:** Figure S5 continued, related to Figure 2.

365 **Figure S12:** Total counts of loss-of-function alleles standardized by the total counts of modifier  
366 alleles for each hybrid individual ordered by proportion of domestic goat (indicated in  
367 parentheses), related to Figure 4.

368

369 **Document S2** contains Tables S1-S13.

370 **Table S1:** Genome contiguity statistics of the draft and scaffolded Alpine ibex assemblies, related  
371 to Figure 1.

372 **Table S2:** Summary of repeat annotations, related to Figure 1.

373 **Table S3:** BUSCO statistics for the scaffolded assembly and the protein-coding gene annotation  
374 of Alpine ibex, related to Figure 1.

375 **Table S4:** Genome annotation stats, related to Figure 1.

376 **Table S5:** Syntenic blocks identified in the GENESPACE analysis, related to Figure 1.

377 **Table S6:** Gene orthogroups identified in the GENESPACE analysis, related to Figure 1.

378 **Table S7:** Goat and goat/ibex hybrid individuals sequenced in the present study, related to  
379 Figures 2-4.

380 **Table S8:** Number of effects of genetic variants by type, related to Figure 4.

381 **Table S9:** Number of effects of genetic variants by region, related to Figure 4.

382 **Table S10:** Summary of deleterious mutations' PFAM annotations, related to Figure 4.

383 **Table S11:** Newly acquired loss-of-function (LOF) variants and candidates for heterosis, related  
384 to Figure 4.

385 **Table S12:** Summary of the ONT runs used for genome assembly, related to Figure 1.

386 **Table S13:** Species and IDs of the available datasets used in this study, related to Figures 3 and  
387 4.

388

389 **Document S3** Supplementary Text

390

## 391 **Figure legends**

392 **Figure 1: Sampling and genome description.** A) Picture of a female Alpine ibex with her  
393 offspring (photo by Dario de Siena, Archivio PNGP). B) Map of species distribution and zoom in  
394 on the sampling location of Odissea (shown in yellow), the hybrids (green), and domestic goats  
395 (blue). C) Snail plot visualizing assembly statistics: scaffold statistics, sequence composition  
396 proportions, and BUSCO completeness scores. D) Riparian plot showing the results of the gene  
397 synteny analysis conducted on the cattle, sheep, domestic goat, and Alpine ibex genomes using  
398 GENESPACE. The human genome was used as an outgroup. See also Figures S1-S4.

399

400 **Figure 2: Conserved synteny at the MHC and high diversity in hybrids.** A) Close-up of the  
401 synteny analysis, conducted with GENESPACE, highlighting two MHC regions within Alpine ibex  
402 chromosome 23 (light blue and orange, respectively).

403 B) Structural variation along chromosome 23 based on SyRI, including annotations of domestic  
404 goat (top) and Alpine ibex (bottom) in the range encompassing the major MHC II region.

405 C) Average individual heterozygosity is shown as observed heterozygosity in Alpine ibex (blue),  
406 domestic goat (orange), and hybrids (purple). Heterozygosity excess and deficit in hybrids were  
407 shown with green (positive values) and orange (negative values), respectively. The grey box  
408 highlights a region corresponding to 25.47-25.55 Mb (encoding *DQA* and *DQB*), which showed a  
409 local lack of coverage in domestic goats while being evenly covered in Alpine ibex (except for  
410 Alpine ibex individuals with previously reported historic introgression in the MHC region, see  
411 Figures S5-11 and Grossen et al. <sup>30</sup>).

412

413 **Figure 3: Genome-wide patterns of hybridization**

414 A) Picture of hybrid individual 10. B) Picture of hybrid individual 8. C) Principal Component  
415 Analysis of biallelic autosomal SNPs showing the clustering of species and the distribution of  
416 hybrids along the conjunction between Alpine ibex and domestic goat/bezoar. D) Chromosome  
417 paintings drawn with Mosaic, ordered according to the proportion of domestic goat ancestry  
418 (decreasing proportion of goat genome shown in orange from left to right).

419

420 **Figure 4: Deleterious mutation load in hybrids**

421 A) Phylogenetic tree showing species relationships and the definition of “goat-load” and “ibex-  
422 load” defined as newly derived mutations private to the respective species. B) Counts of loss-of-  
423 function alleles found in the heterozygous state for each sequenced hybrid individual (ordered  
424 according to proportion of goat). C) Total counts of loss-of-function alleles standardized by the  
425 total counts of modifier alleles. Box plots per species. Local domestic goat refers to breeds kept  
426 in the region where hybrid swarms were detected. See also Figure S12. D) Masked loss-of-  
427 function load (heterozygote counts) per individual. New goats, as in C.

428

429

430 **Methods**

431 We collected fresh samples from thirteen individuals: one female Alpine ibex (Odissea), eight  
432 hybrids, and four domestic goats. For the female Alpine ibex, we extracted multiple organs and  
433 performed high molecular weight DNA extractions to enable Oxford Nanopore Technologies  
434 (ONT; Oxford, UK) long-read (including ultra-long) and Illumina NovaSeq 6000 short-read  
435 sequencing (Table S12). These data were used to produce a draft genome assembly, which was  
436 then integrated with Hi-C sequencing data from the same individual's liver. The samples from the  
437 other individuals were prepared for whole-genome paired-end sequencing on an Illumina  
438 NovaSeq 6000. Detailed protocols are provided in the [Supplementary Text](#).

439

#### 440 **Genome assembly and evaluation**

441 We assembled the ONT data into a draft genome using Flye v2.9<sup>54</sup>, after which short-read data  
442 were aligned and used for polishing with Pilon v1.23<sup>55</sup>. We scanned the assembly for laboratory  
443 or environmental contaminants using the NCBI Foreign Contamination Screen tool<sup>56</sup>. Following  
444 quality filtering, we mapped Hi-C reads following the Arima Genomics pipeline  
445 ([https://github.com/ArimaGenomics/mapping\\_pipeline](https://github.com/ArimaGenomics/mapping_pipeline)) and performed scaffolding with YaHS  
446 v1.1<sup>57</sup>. Finally, we evaluated the final assembly for contiguity, k-mer completeness, reference-  
447 free QV, and expected gene content (further methodological details are in the [Supplementary](#)  
448 [Text](#)). Genome assembly statistics were visualized with a snail plot in BlobToolKit v4.3.2<sup>58</sup> (Figure  
449 1C).

450

#### 451 **Gene model prediction, curation, and functional annotation**

452 We softmasked the Alpine ibex genome by merging repeat coordinates identified via  
453 RepeatModeler v2.0.3<sup>59</sup> and TRF<sup>60</sup>. Then we incorporated RNA-seq and homology-based  
454 evidence into the braker2 v2.1.6 pipeline<sup>61-69</sup> using pre-trained parameter sets for human (*Homo*  
455 *sapiens*), which is the evolutionarily closest taxon for Alpine ibex available within the software.  
456 Subsequently, an annotation lift-over from the sheep reference genome [ARS-UI\_Ramb\_v2.0,  
457 NCBI Genome GCF\_016772045.1<sup>70,71</sup>] was conducted with Liftoff v1.6.3<sup>72</sup>. In order to reduce  
458 the redundancy of the transcript set obtained, we employed an isoform pruning pipeline as  
459 previously described<sup>73</sup>. Finally, gene models were annotated using eggNOG mapper v2.1.11<sup>74</sup>  
460 in DIAMOND-search mode. The details of used external evidence for gene prediction and the  
461 detailed methodology can be found in the [Supplementary Text](#). Functional annotation of the gene  
462 models showed that 54,205 out of 61,420 (88.2%) transcripts had matches in the eggNOG protein  
463 database (corresponding to 81.1% of genes).

464 The mitochondrial genome encodes 13 proteins, including seven complex I proteins (ND1-3,  
465 ND4L, ND4-6), four complex IV proteins (COXI, COXII, COXIII, and CytB), and 2 ATP synthase  
466 subunits (ATPase 6 and 8; Figure S2).

467

### 468 **Synteny analysis and structural rearrangement identification**

469 We ran GENESPACE v1.2.3 <sup>75</sup> with default parameters to examine synteny among the Alpine  
470 ibex genome and the human (GRCh38.p14), cattle (ARS-UCD1.3), sheep (ARS-UI\_Ramb\_v2.0),  
471 and domestic goat (ARS1.2, GCF\_001704415.2) references, focusing on primary chromosome  
472 scaffolds. We further explored syntenic regions and structural rearrangements between domestic  
473 goat and Alpine ibex reference genomes with SyRI v1.6.3 <sup>76</sup> (see [Supplementary Text](#)). Results  
474 were visualized using plotsr v1.1.1 <sup>77</sup>.

475

### 476 **SNP genotyping and hybridization analyses**

477 Whole-genome sequencing data from eight newly sequenced hybrids and goats were combined  
478 with available datasets for Alpine ibex (N=29), domestic goat (N=18), bezoar (N=4), Iberian ibex  
479 (N=4), Nubian ibex (N=2), Siberian ibex (N=2), and markhor (N=1), plus four outgroup samples  
480 (chamois, cattle, sheep, bighorn sheep; see Table S13) After alignment to the new Alpine ibex  
481 genome following the *germline* pipeline of the NVIDIA Clara Parabricks v3.8 <sup>78</sup>, variants were  
482 called, and hard filtering was performed with GATK v4.1.0 <sup>79</sup>. Eventually, we retained SNPs  
483 polymorphic among *Capra* spp. (see Supplementary Text for selection criteria), which were  
484 autosomal, bi-allelic, with a minimal genotype quality of 20 and a minimal genotyping rate of 80%  
485 using bcftools v1.2 <sup>80</sup>. We estimated average per-site heterozygosity with VCFtools <sup>81</sup> and used  
486 PLINK v2.0 <sup>82</sup> for principal component analysis. After data phasing using beagle v22Jul22.46e <sup>83</sup>,  
487 the Mosaic R-toolbox <sup>84</sup> was employed to examine Alpine ibex and goat haplotypes in hybrids;  
488 chromosome painting was visualized via the karyogram function. Finally, putative functional  
489 changes were annotated with SnpEff v4.3t <sup>85</sup>. Individual (derived) genetic load was computed as  
490 masked LOF load (number of heterozygotes) or total load (number of heterozygotes + 2\* number  
491 of homozygotes) and standardized by the respective numbers of MODIFIER genotypes. These  
492 standardized estimates of LOF load in domestic goat vs. Alpine ibex were then compared using  
493 a Welch two-sample t-test (see also [Supplementary Text](#)).

494

## 495 **References**

496 1. Bongaarts, J. (2019). IPBES, 2019. Summary for policymakers of the global assessment

- 497 report on biodiversity and ecosystem services of the Intergovernmental Science-Policy  
498 Platform on Biodiversity and Ecosystem Services. Preprint,  
499 <https://doi.org/10.1111/padr.12283> <https://doi.org/10.1111/padr.12283>.
- 500 2. Dussex, N., Morales, H.E., Grossen, C., Dalén, L., and van Oosterhout, C. (2023). Purging  
501 and accumulation of genetic load in conservation. *Trends Ecol. Evol.* *38*, 961–969.
- 502 3. Robinson, J., Kyriazis, C.C., Yuan, S.C., and Lohmueller, K.E. (2023). Deleterious variation  
503 in natural populations and implications for conservation genetics. *Annu. Rev. Anim. Biosci.*  
504 *11*, 93–114.
- 505 4. Xue, Y., Prado-Martinez, J., Sudmant, P.H., Narasimhan, V., Ayub, Q., Szpak, M.,  
506 Frandsen, P., Chen, Y., Yngvadottir, B., Cooper, D.N., et al. (2015). Mountain gorilla  
507 genomes reveal the impact of long-term population decline and inbreeding. *Science* *348*,  
508 242–245.
- 509 5. Grossen, C., Guillaume, F., Keller, L.F., and Croll, D. (2020). Purging of highly deleterious  
510 mutations through severe bottlenecks in Alpine ibex. *Nat. Commun.* *11*, 1001.
- 511 6. Dussex, N., van der Valk, T., Morales, H.E., Wheat, C.W., Díez-Del-Molino, D., von Seth,  
512 J., Foster, Y., Kutschera, V.E., Guschanski, K., Rhie, A., et al. (2021). Population genomics  
513 of the critically endangered kākāpō. *Cell Genom.* *1*, 100002.
- 514 7. Whitlock, M.C., and Davis, B. (2011). Genetic Load. eLS.  
515 <https://doi.org/10.1002/9780470015902.a0001787.pub2>.
- 516 8. Kardos, M., Zhang, Y., Parsons, K.M., A, Y., Kang, H., Xu, X., Liu, X., Matkin, C.O., Zhang,  
517 P., Ward, E.J., et al. (2023). Inbreeding depression explains killer whale population  
518 dynamics. *Nat. Ecol. Evol.* *7*, 675–686.
- 519 9. Stoffel, M.A., Johnston, S.E., Pilkington, J.G., and Pemberton, J.M. (2024). Purifying and  
520 balancing selection on embryonic semi-lethal haplotypes in a wild mammal. *Evol. Lett.* *8*,  
521 222–230.
- 522 10. Genovart, M. (2009). Natural hybridization and conservation. *Biodivers. Conserv.* *18*, 1435–  
523 1439.
- 524 11. Mallet, J. (2005). Hybridization as an invasion of the genome. *Trends Ecol. Evol.* *20*, 229–  
525 237.
- 526 12. Moran, B.M., Payne, C., Langdon, Q., Powell, D.L., Brandvain, Y., and Schumer, M. (2021).  
527 The genomic consequences of hybridization. *Elife* *10*. <https://doi.org/10.7554/eLife.69016>.
- 528 13. Barton, N.H. (2001). The role of hybridization in evolution. *Mol. Ecol.* *10*, 551–568.
- 529 14. Burke, J.M., and Arnold, M.L. (2001). Genetics and the fitness of hybrids. *Annu. Rev.*  
530 *Genet.* *35*, 31–52.
- 531 15. Allendorf, F.W., Leary, R.F., Spruell, P., and Wenburg, J.K. (2001). The problems with  
532 hybrids: setting conservation guidelines. *Trends Ecol. Evol.* *16*, 613–622.
- 533 16. Leitwein, M., Cayuela, H., Ferchaud, A.-L., Normandeau, É., Gagnaire, P.-A., and

- 534 Bernatchez, L. (2019). The role of recombination on genome-wide patterns of local  
535 ancestry exemplified by supplemented brook charr populations. *Mol. Ecol.* *28*, 4755–4769.
- 536 17. Schumer, M., Xu, C., Powell, D.L., Durvasula, A., Skov, L., Holland, C., Blazier, J.C.,  
537 Sankararaman, S., Andolfatto, P., Rosenthal, G.G., et al. (2018). Natural selection interacts  
538 with recombination to shape the evolution of hybrid genomes. *Science* *360*, 656–660.
- 539 18. Simon, M.F., Mendoza Flores, J.M., Liu, H.-L., Martins, M.L.L., Drovetski, S.V.,  
540 Przelomska, N.A.S., Loiselle, H., Cavalcanti, T.B., Inglis, P.W., Mueller, N.G., et al. (2022).  
541 Phylogenomic analysis points to a South American origin of Manihot and illuminates the  
542 primary gene pool of cassava. *New Phytol.* *233*, 534–545.
- 543 19. Wang, L., Beissinger, T.M., Lorant, A., Ross-Ibarra, C., Ross-Ibarra, J., and Hufford, M.B.  
544 (2017). The interplay of demography and selection during maize domestication and  
545 expansion. *Genome Biol.* *18*, 215.
- 546 20. Janzen, G.M., Wang, L., and Hufford, M.B. (2019). The extent of adaptive wild introgression  
547 in crops. *New Phytol.* *221*, 1279–1288.
- 548 21. Liu, S., Zhang, L., Sang, Y., Lai, Q., Zhang, X., Jia, C., Long, Z., Wu, J., Ma, T., Mao, K., et  
549 al. (2022). Demographic history and natural selection shape patterns of deleterious  
550 mutation load and barriers to introgression across *Populus* genome. *Mol. Biol. Evol.* *39*.  
551 <https://doi.org/10.1093/molbev/msac008>.
- 552 22. Theissinger, K., Fernandes, C., Formenti, G., Bista, I., Berg, P.R., Bleidorn, C., Bombarely,  
553 A., Crottini, A., Gallo, G.R., Godoy, J.A., et al. (2023). How genomics can help biodiversity  
554 conservation. *Trends Genet.* *39*, 545–559.
- 555 23. Stüwe, M., and Nievergelt, B. (1991). Recovery of alpine ibex from near extinction: the  
556 result of effective protection, captive breeding, and reintroductions. *Appl. Anim. Behav. Sci.*  
557 *29*, 379–387.
- 558 24. Brambilla, A., Zehnder, N., Bassano, B., Rossi, L., and Grossen, C. (2024). Genetic  
559 evidence of a hybrid swarm between Alpine ibex (*Capra ibex*) and domestic goat (*C.*  
560 *hircus*). *Evol. Appl.* *17*, e13761.
- 561 25. Brambilla, A., Von Hardenberg, A., Nelli, L., and Bassano, B. (2020). Distribution, status,  
562 and recent population dynamics of Alpine ibex *Capra ibex* in Europe. *Mamm. Rev.* *50*, 267–  
563 277.
- 564 26. Biebach, I., and Keller, L.F. (2010). Inbreeding in reintroduced populations: the effects of  
565 early reintroduction history and contemporary processes. *Conserv. Genet.* *11*, 527–538.
- 566 27. Brambilla, A., Biebach, I., Bassano, B., Bogliani, G., and von Hardenberg, A. (2015). Direct  
567 and indirect causal effects of heterozygosity on fitness-related traits in Alpine ibex. *Proc.*  
568 *Biol. Sci.* *282*, 20141873.
- 569 28. Bozzuto, C., Biebach, I., Muff, S., Ives, A.R., and Keller, L.F. (2019). Inbreeding reduces  
570 long-term growth of Alpine ibex populations. *Nat Ecol Evol* *3*, 1359–1364.
- 571 29. Mürger, X., Robin, M., Dalén, L., and Grossen, C. (2024). Facilitated introgression from  
572 domestic goat into Alpine ibex at immune loci. *Mol. Ecol.*, e17429.

- 573 30. Grossen, C., Keller, L., Biebach, I., International Goat Genome Consortium, and Croll, D.  
574 (2014). Introgression from domestic goat generated variation at the major histocompatibility  
575 complex of Alpine ibex. *PLoS Genet.* *10*, e1004438.
- 576 31. Moroni, B., Brambilla, A., Rossi, L., Meneguz, P.G., Bassano, B., and Tizzani, P. (2022).  
577 Hybridization between Alpine Ibex and Domestic Goat in the Alps: A Sporadic and  
578 Localized Phenomenon? *Animals (Basel)* *12*. <https://doi.org/10.3390/ani12060751>.
- 579 32. Bickhart, D.M., Rosen, B.D., Koren, S., Sayre, B.L., Hastie, A.R., Chan, S., Lee, J., Lam,  
580 E.T., Liachko, I., Sullivan, S.T., et al. (2017). Single-molecule sequencing and chromatin  
581 conformation capture enable de novo reference assembly of the domestic goat genome.  
582 *Nat. Genet.* *49*, 643–650.
- 583 33. Piertney, S.B., and Oliver, M.K. (2006). The evolutionary ecology of the major  
584 histocompatibility complex. *Heredity* *96*, 7–21.
- 585 34. Jain, M., Koren, S., Miga, K.H., Quick, J., Rand, A.C., Sasani, T.A., Tyson, J.R., Beggs,  
586 A.D., Dilthey, A.T., Fiddes, I.T., et al. (2018). Nanopore sequencing and assembly of a  
587 human genome with ultra-long reads. *Nat. Biotechnol.* *36*, 338–345.
- 588 35. Koren, S., Rhie, A., Walenz, B.P., Dilthey, A.T., Bickhart, D.M., Kingan, S.B., Hiendleder,  
589 S., Williams, J.L., Smith, T.P.L., and Phillippy, A.M. (2018). De novo assembly of  
590 haplotype-resolved genomes with trio binning. *Nat. Biotechnol.*  
591 <https://doi.org/10.1038/nbt.4277>.
- 592 36. Chin, C.-S., Wagner, J., Zeng, Q., Garrison, E., Garg, S., Fungtammasan, A., Rautiainen,  
593 M., Aganezov, S., Kirsche, M., Zarate, S., et al. (2020). A diploid assembly-based  
594 benchmark for variants in the major histocompatibility complex. *Nat. Commun.* *11*, 4794.
- 595 37. Beck, S., and Trowsdale, J. (1999). Sequence organisation of the class II region of the  
596 human MHC. *Immunol. Rev.* *167*, 201–210.
- 597 38. Kelley, J., Walter, L., and Trowsdale, J. (2005). Comparative genomics of major  
598 histocompatibility complexes. *Immunogenetics* *56*, 683–695.
- 599 39. Gowane, G., Vandre, R., Nangre, M., and Sharma, A. (2014). Major histocompatibility  
600 complex (MHC) of bovines: an insight into infectious disease resistance. *Livestock*  
601 *Research International*, *1*, 46–57.
- 602 40. Westerdahl, H. (2007). Passerine MHC: genetic variation and disease resistance in the  
603 wild. *J. Ornithol.* *148*, 469–477.
- 604 41. Hedrick, P.W., Kim, T.J., and Parker, K.M. (2001). Parasite resistance and genetic variation  
605 in the endangered Gila topminnow. *Animal Conservation forum* *4*, 103–109.
- 606 42. Hedrick, P.W., Parker, K.M., Miller, E.L., and Miller, P.S. (1999). Major histocompatibility  
607 complex variation in the endangered Przewalski's horse. *Genetics* *152*, 1701–1710.
- 608 43. Paterson, S., Wilson, K., and Pemberton, J.M. (1998). Major histocompatibility complex  
609 variation associated with juvenile survival and parasite resistance in a large unmanaged  
610 ungulate population (*Ovis aries* L.). *Proceedings of the National Academy of Sciences* *95*,  
611 3714–3719.

- 612 44. Langefors, A., Lohm, J., Grahn, M., Andersen, O., and von Schantz, T. (2001). Association  
613 between major histocompatibility complex class IIB alleles and resistance to *Aeromonas*  
614 *salmonicida* in Atlantic salmon. *Proc. Biol. Sci.* 268, 479–485.
- 615 45. Fu, M., Eimes, J.A., Kong, S., Lamichhaney, S., and Waldman, B. (2023). Identification of  
616 major histocompatibility complex genotypes associated with resistance to an amphibian  
617 emerging infectious disease. *Infect. Genet. Evol.* 113, 105470.
- 618 46. Brambilla, A., Keller, L., Bassano, B., and Grossen, C. (2018). Heterozygosity-fitness  
619 correlation at the major histocompatibility complex despite low variation in Alpine ibex (  
620 *Capra ibex*). *Evol. Appl.* 11, 631–644.
- 621 47. Chen, Z.J. (2013). Genomic and epigenetic insights into the molecular bases of heterosis.  
622 *Nat. Rev. Genet.* 14, 471–482.
- 623 48. Garcia-Erill, G., Liu, S., Le, M.D., Hurley, M.M., Nguyen, H.D., Nguyen, D.Q., Nguyen, D.H.,  
624 Santander, C.G., Sánchez Barreiro, F., Gomes Martins, N.F., et al. (2025). Genomes of  
625 critically endangered saola are shaped by population structure and purging. *Cell*.  
626 <https://doi.org/10.1016/j.cell.2025.03.040>.
- 627 49. Henn, B.M., Botigué, L.R., Peischl, S., Dupanloup, I., Lipatov, M., Maples, B.K., Martin,  
628 A.R., Musharoff, S., Cann, H., Snyder, M.P., et al. (2016). Distance from sub-Saharan  
629 Africa predicts mutational load in diverse human genomes. *Proc. Natl. Acad. Sci. U. S. A.*  
630 113, E440–E449.
- 631 50. Khan, A., Patel, K., Shukla, H., Viswanathan, A., van der Valk, T., Borthakur, U., Nigam, P.,  
632 Zachariah, A., Jhala, Y., Kardos, M., et al. (2021). Genomic evidence for inbreeding  
633 depression and purging of deleterious genetic variation in Indian tigers. *bioRxiv*.  
634 <https://doi.org/10.1101/2021.05.18.444660>.
- 635 51. Ochoa, A., and Gibbs, H.L. (2021). Genomic signatures of inbreeding and mutation load in  
636 a threatened rattlesnake. *Mol. Ecol.* 30, 5454–5469.
- 637 52. Kleinman-Ruiz, D., Lucena-Perez, M., Villanueva, B., Fernández, J., Saveljev, A.P.,  
638 Ratkiewicz, M., Schmidt, K., Galtier, N., García-Dorado, A., and Godoy, J.A. (2022).  
639 Purging of deleterious burden in the endangered Iberian lynx. *Proc. Natl. Acad. Sci. U. S.*  
640 *A.* 119, e2110614119.
- 641 53. Ottenburghs, J. (2021). The genic view of hybridization in the Anthropocene. *Evol. Appl.* 14,  
642 2342–2360.
- 643 54. Kolmogorov, M., Yuan, J., Lin, Y., and Pevzner, P.A. (2019). Assembly of long, error-prone  
644 reads using repeat graphs. *Nat. Biotechnol.* 37, 540–546.
- 645 55. Walker, B.J., Abeel, T., Shea, T., Priest, M., Abouelliel, A., Sakthikumar, S., Cuomo, C.A.,  
646 Zeng, Q., Wortman, J., Young, S.K., et al. (2014). Pilon: an integrated tool for  
647 comprehensive microbial variant detection and genome assembly improvement. *PLoS One*  
648 9, e112963.
- 649 56. Astashyn, A., Tvedte, E.S., Sweeney, D., Sapojnikov, V., Bouk, N., Joukov, V., Mozes, E.,  
650 Strope, P.K., Sylla, P.M., Wagner, L., et al. (2024). Rapid and sensitive detection of  
651 genome contamination at scale with FCS-GX. *Genome Biol.* 25, 60.

- 652 57. Zhou, C., McCarthy, S.A., and Durbin, R. (2023). YaHS: yet another Hi-C scaffolding tool.  
653 *Bioinformatics* 39, btac808.
- 654 58. Challis, R., Richards, E., Rajan, J., Cochrane, G., and Blaxter, M. (2020). BlobToolKit--  
655 interactive quality assessment of genome assemblies. *G3: Genes, Genomes, Genetics* 10,  
656 1361–1374.
- 657 59. Flynn, J.M., Hubley, R., Goubert, C., Rosen, J., Clark, A.G., Feschotte, C., and Smit, A.F.  
658 (2020). RepeatModeler2 for automated genomic discovery of transposable element  
659 families. *Proc. Natl. Acad. Sci. U. S. A.* 117, 9451–9457.
- 660 60. Benson, G. (1999). Tandem repeats finder: a program to analyze DNA sequences. *Nucleic  
661 Acids Res.* 27, 573–580.
- 662 61. Brůna, T., Hoff, K.J., Lomsadze, A., Stanke, M., and Borodovsky, M. (2021). BRAKER2:  
663 automatic eukaryotic genome annotation with GeneMark-EP+ and AUGUSTUS supported  
664 by a protein database. *NAR Genom Bioinform* 3, lqaa108.
- 665 62. Hoff, K.J., Lomsadze, A., Borodovsky, M., and Stanke, M. (2019). Whole-genome  
666 annotation with BRAKER. *Methods Mol. Biol.* 1962, 65–95.
- 667 63. Hoff, K.J., Lange, S., Lomsadze, A., Borodovsky, M., and Stanke, M. (2016). BRAKER1:  
668 Unsupervised RNA-seq-based genome annotation with GeneMark-ET and AUGUSTUS.  
669 *Bioinformatics* 32, 767–769.
- 670 64. Stanke, M., Diekhans, M., Baertsch, R., and Haussler, D. (2008). Using native and  
671 syntenically mapped cDNA alignments to improve de novo gene finding. *Bioinformatics* 24,  
672 637–644.
- 673 65. Stanke, M., Schöffmann, O., Morgenstern, B., and Waack, S. (2006). Gene prediction in  
674 eukaryotes with a generalized hidden Markov model that uses hints from external sources.  
675 *BMC Bioinformatics* 7, 62.
- 676 66. Buchfink, B., Xie, C., and Huson, D.H. (2015). Fast and sensitive protein alignment using  
677 DIAMOND. *Nat. Methods* 12, 59–60.
- 678 67. Li, H., Handsaker, B., Wysoker, A., Fennell, T., Ruan, J., Homer, N., Marth, G., Abecasis,  
679 G., Durbin, R., and 1000 Genome Project Data Processing Subgroup (2009). The  
680 Sequence Alignment/Map format and SAMtools. *Bioinformatics* 25, 2078–2079.
- 681 68. Barnett, D.W., Garrison, E.K., Quinlan, A.R., Strömberg, M.P., and Marth, G.T. (2011).  
682 BamTools: a C++ API and toolkit for analyzing and managing BAM files. *Bioinformatics* 27,  
683 1691–1692.
- 684 69. Lomsadze, A., Burns, P.D., and Borodovsky, M. (2014). Integration of mapped RNA-Seq  
685 reads into automatic training of eukaryotic gene finding algorithm. *Nucleic Acids Res.* 42,  
686 e119.
- 687 70. International Sheep Genomics Consortium, Archibald, A.L., Cockett, N.E., Dalrymple, B.P.,  
688 Faraut, T., Kijas, J.W., Maddox, J.F., McEwan, J.C., Hutton Oddy, V., Raadsma, H.W., et  
689 al. (2010). The sheep genome reference sequence: a work in progress. *Anim. Genet.* 41,  
690 449–453.

- 691 71. Li, R., Yang, P., Li, M., Fang, W., Yue, X., Nanaei, H.A., Gan, S., Du, D., Cai, Y., Dai, X., et  
692 al. (2021). A Hu sheep genome with the first ovine Y chromosome reveal introgression  
693 history after sheep domestication. *Sci. China Life Sci.* *64*, 1116–1130.
- 694 72. Shumate, A., and Salzberg, S.L. (2021). Liftoff: accurate mapping of gene annotations.  
695 *Bioinformatics* *37*, 1639–1643.
- 696 73. Ivankovic, M., Brand, J.N., Pandolfini, L., Brown, T., Pippel, M., Rozanski, A., Schubert, T.,  
697 Grohme, M.A., Winkler, S., Robledillo, L., et al. (2023). A comparative analysis of planarian  
698 genomes reveals regulatory conservation in the face of rapid structural divergence. *bioRxiv*.  
699 <https://doi.org/10.1101/2023.12.22.572568>.
- 700 74. Cantalapiedra, C.P., Hernández-Plaza, A., Letunic, I., Bork, P., and Huerta-Cepas, J.  
701 (2021). eggNOG-mapper v2: Functional Annotation, Orthology Assignments, and Domain  
702 Prediction at the Metagenomic Scale. *Mol. Biol. Evol.* *38*, 5825–5829.
- 703 75. Lovell, J.T., Sreedasyam, A., Schranz, M.E., Wilson, M., Carlson, J.W., Harkess, A., Emms,  
704 D., Goodstein, D.M., and Schmutz, J. (2022). GENESPACE tracks regions of interest and  
705 gene copy number variation across multiple genomes. *Elife* *11*.  
706 <https://doi.org/10.7554/eLife.78526>.
- 707 76. Goel, M., Sun, H., Jiao, W.-B., and Schneeberger, K. (2019). SyRI: finding genomic  
708 rearrangements and local sequence differences from whole-genome assemblies. *Genome*  
709 *Biol.* *20*, 277.
- 710 77. Goel, M., and Schneeberger, K. (2022). plotsr: visualizing structural similarities and  
711 rearrangements between multiple genomes. *Bioinformatics* *38*, 2922–2926.
- 712 78. Franke, K.R., and Crowgey, E.L. (2020). Accelerating next generation sequencing data  
713 analysis: an evaluation of optimized best practices for Genome Analysis Toolkit algorithms.  
714 *Genomics Inform.* *18*, e10.
- 715 79. McKenna, A., Hanna, M., Banks, E., Sivachenko, A., Cibulskis, K., Kernytsky, A.,  
716 Garimella, K., Altshuler, D., Gabriel, S., Daly, M., et al. (2010). The Genome Analysis  
717 Toolkit: a MapReduce framework for analyzing next-generation DNA sequencing data.  
718 *Genome Res.* *20*, 1297–1303.
- 719 80. Danecek, P., Bonfield, J.K., Liddle, J., Marshall, J., Ohan, V., Pollard, M.O., Whitwham, A.,  
720 Keane, T., McCarthy, S.A., Davies, R.M., et al. (2021). Twelve years of SAMtools and  
721 BCFtools. *Gigascience* *10*, giab008.
- 722 81. Danecek, P., Auton, A., Abecasis, G., Albers, C.A., Banks, E., DePristo, M.A., Handsaker,  
723 R.E., Lunter, G., Marth, G.T., Sherry, S.T., et al. (2011). The variant call format and  
724 VCFtools. *Bioinformatics* *27*, 2156–2158.
- 725 82. Chang, C.C., Chow, C.C., Tellier, L.C., Vattikuti, S., Purcell, S.M., and Lee, J.J. (2015).  
726 Second-generation PLINK: rising to the challenge of larger and richer datasets.  
727 *Gigascience* *4*, 7.
- 728 83. Browning, B.L., Tian, X., Zhou, Y., and Browning, S.R. (2021). Fast two-stage phasing of  
729 large-scale sequence data. *Am. J. Hum. Genet.* *108*, 1880–1890.

- 730 84. Salter-Townshend, M., and Myers, S. (2019). Fine-Scale Inference of Ancestry Segments  
731 Without Prior Knowledge of Admixing Groups. *Genetics* 212, 869–889.
- 732 85. Cingolani, P., Platts, A., Wang, L.L., Coon, M., Nguyen, T., Wang, L., Land, S.J., Lu, X.,  
733 and Ruden, D.M. (2012). A program for annotating and predicting the effects of single  
734 nucleotide polymorphisms, SnpEff: SNPs in the genome of *Drosophila melanogaster* strain  
735 w11118; iso-2; iso-3. *Fly* 6, 80–92.